

# Density dependent spin susceptibility and effective mass in interacting quasi-two dimensional electron systems

Ying Zhang and S. Das Sarma  
Condensed Matter Theory Center, Department of Physics,  
University of Maryland, College Park, MD 20742-4111  
(Dated: April 11, 2018)

Motivated by recent experimental reports, we carry out a Fermi liquid many-body calculation of the interaction induced renormalization of the spin susceptibility and effective mass in realistic two dimensional (2D) electron systems as a function of carrier density using the leading-order 'ladder-bubble' expansion in the dynamically screened Coulomb interaction. Using realistic material parameters for various semiconductor-based 2D systems, we find reasonable quantitative agreement with recent experimental susceptibility and effective mass measurements. We point out a number of open questions regarding quantitative aspects of the comparison between theory and experiment in low-density 2D electron systems.

PACS numbers: 71.10.-w; 71.10.Ca; 73.20.Mf; 73.40.-c

## I. INTRODUCTION

It is well-known that the mutual Coulomb interaction between electrons could cause substantial quantitative modification of thermodynamic properties (e.g. effective mass, specific heat, compressibility, magnetic susceptibility) in an interacting electron liquid. This is the so-called many-body renormalization of the Fermi liquid parameters, which has been studied extensively in three dimensional metals<sup>1</sup> and in two dimensional (2D) semiconductor structures<sup>2</sup> for a very long time. At zero temperature (or more generally at low temperatures,  $T/T_F \ll 1$  where  $T_F = E_F/k_B$  is the Fermi temperature) the many-body Fermi liquid renormalization for a quantum electronic system is entirely determined by the electron density ( $n$ ) with the dimensionless density parameter  $r_s$  being defined as the average inter-electron separation measured in the units of Bohr radius:  $r_s \equiv (\pi n)^{-1/2}/a_B$  where  $a_B = \kappa \hbar^2/(me^2)$  is the effective Bohr radius for a background (lattice) dielectric constant  $\kappa$  and a band mass  $m$  – this definition of  $r_s$  applies to 2D (in 3D:  $r_s \propto n^{-1/3}$ ) with  $n$  being the 2D electron density. It is easy to see that our  $r_s$ -parameter is proportional to the ratio of the average Coulomb potential energy (i.e. the interaction energy) to the noninteracting kinetic energy, and as such the system is strongly interacting at large  $r_s$  (low density) and weakly interacting at small  $r_s$  (high density). We emphasize that our definition of  $r_s$  does not depend on the spin (or valley degeneracy in 2D) of the system. Studying (and comparing theory with experiment) the density dependence of various Fermi liquid parameters in interacting electron liquids has been one of the most important and active many-body research areas in condensed matter physics in 3D metallic systems (as well as in normal He-3, a quintessential Fermi liquid albeit with a *short-range* inter-particle interaction) and more recently, in 2D electron systems confined in semiconductor structures. The 2D systems have the distinct advantage of the density being a tunable parameter so that the density dependence of the Fermi liquid renormalization

can be studied directly. In this paper, we theoretically consider the density-dependent many-body renormalization of the 2D electronic spin susceptibility and effective mass, a subject of considerable recent experimental activity<sup>3,4,5,6,7,8,9,10,11</sup> in a number of different semiconductor heterostructures with confined 2D electron systems.

There has been a number of experimental papers appearing in the recent literature reporting the low-temperature ( $\lesssim 100\text{mK}$ ) measurement of the susceptibility<sup>3,4,5,6,7,8,9</sup> and effective mass<sup>10,11</sup> in 2D electron systems as a function of carrier density in the  $r_s \approx 1 - 10$  parameter range. Although some aspects of the data in different experiments (and more importantly, the interpretation of the data) have been controversial – most especially on the issue of whether there is a spontaneous density-driven ferromagnetic spin polarization transition at low carrier densities in 2D systems – the experimental reports convincingly establish a strong enhancement in both the spin susceptibility and effective mass as a function of decreasing (increasing) carrier density  $n$  (interaction parameter  $r_s$ ). This strong enhancement of the susceptibility with decreasing carrier density has been demonstrated in 2D electron systems confined in (100) Si inversion layers, in GaAs heterostructures, and in AlAs quantum wells. The typical enhancement in the low temperature susceptibility is in the range of a factor of 1 – 4 for  $r_s \approx 1 - 10$ . In addition to the strong low-density enhancement of the measured low-temperature susceptibility, there are several other interesting and intriguing features in the experiments. The susceptibility enhancement shows a modest dependence on the induced spin polarization (or equivalently, a change in the spin degeneracy) in the 2D system – since the susceptibility is typically measured<sup>12</sup> by applying an external magnetic field to produce a spin splitting in the 2D system, the susceptibility is invariably measured in the presence of finite spin polarization (and the extrapolation to zero spin polarization may not always be uniquely reliable). Another interesting observed recent feature, reported in AlAs quantum well systems, is that the susceptibility en-

enhancement is *larger* in the single-valley semiconductor system rather than in the multi-valley system in contrast to the expectation based on just exchange energy considerations (since the multi-valley system is naively expected to be more “dilute” as the electrons are being shared among different valleys). The enhancement of effective mass with decreasing carrier density was observed in Si inversion layer and GaAs heterostructures. This measurement is performed by examining the temperature dependence of the low-temperature Shubnikov de Haas oscillation magnitudes. The effective mass measurement turns out to be more difficult in general. Very recently, a detailed and extremely careful experimental measurement of density dependent effective mass, using several internal consistency checks, has appeared in the literature<sup>11</sup>.

In this paper, we provide an excellent qualitative and reasonable quantitative (realistic) theoretical understanding of the density-dependent 2D spin susceptibility and effective mass measurements at low temperature. Our work, in contrast to much of the existing theoretical literature on the topic, fully incorporates the realistic *quasi*-2D nature of the electron systems (i.e. the fact that these systems have finite widths in the transverse direction normal to the 2D plane of confinement, which considerably modify the Coulomb interaction between the electrons) which is of substantial quantitative importance in the experimental parameter regime. We also study the spin- and the valley-degeneracy dependence of the calculated 2D susceptibility, obtaining in the process qualitative agreement with the recent experimental finding on the anomalous valley dependence of the susceptibility in 2D AIAs quantum well structures. (The spin,  $g_s$  and the valley degeneracy,  $g_v$  dependence of the susceptibility enters through the 2D density of state, which is proportional to  $g_s g_v$ .) Our best quantitative agreement with the experimentally measured 2D effective mass is obtained for the so-called “on-shell” self-energy approximation.

In Sec. II we lay out the theory and formalism of our calculation. We present the calculated results for spin susceptibility in Sec. III and effective mass in Sec. IV for different realistic 2D systems. In the end in Sec. V we discuss upon various issues related to our results and their relations with the experiments.

## II. FORMALISM

We calculate the  $T = 0$  (paramagnetic) spin susceptibility  $\chi^*$  and effective mass  $m^*$  of a *quasi*-2D electron system by using the many-body perturbation theory technique. It has been known<sup>13</sup> for a long time that for an electron system interacting via the Coulomb interaction, the most important terms are associated with the long-range divergence (the so-called ‘ring’ or ‘bubble’ diagrams<sup>13</sup>) of the Coulomb interaction, and as such an expansion in the dynamically screened Coulomb inter-

action (with the screening implemented by the infinite series of ‘bubble’ polarization diagrams) is the appropriate theoretical framework. Such an expansion is, in fact, asymptotically exact in the  $r_s \rightarrow 0$  high-density limit, and is known to work well qualitatively for  $r_s > 1$  although its precise regime of validity can not be determined theoretically and has to be ascertained by comparing with experiments. The theory becomes progressively quantitatively worse as  $r_s$  increases, but unless a quantum phase transition intervenes, there is no specific  $r_s$  value which necessarily limits the qualitative validity of the theory. Motivated by the encouraging fact that this leading-order expansion in the dynamically screened interaction (involving an infinite resummation of all the bubble diagrams in the electron self-energy calculation) seems to provide a good quantitative description<sup>13</sup> for the thermodynamic properties of the 3D simple metals ( $r_s \approx 3 - 6$ ), we apply here the same theory for interacting electrons in *quasi*-2D semiconductor structures.

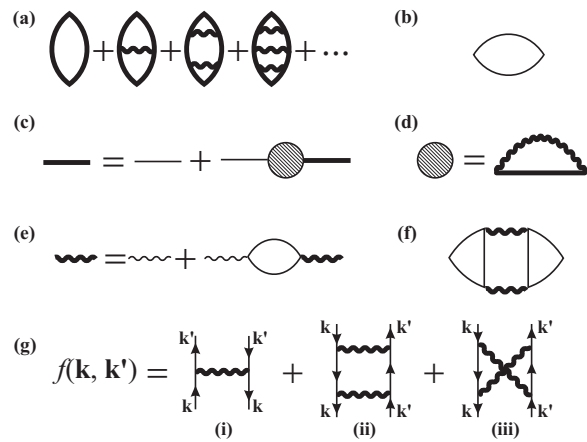


FIG. 1: (Color online.) (a) The RPA ladder-bubble series for the interacting susceptibility with the bold straight line the interacting Green’s function and the bold wavy line the dynamically screened interaction; (b) the noninteracting susceptibility; (c) the Dyson’s equation for the interacting Green’s function in terms of the noninteracting Green’s function and the self-energy; (d) the self-energy in the leading-order expansion in the dynamical screening; (e) the Dyson’s equation for the dynamically screened interaction in terms of the bare Coulomb interaction (thin wavy lines) and the polarization bubble; (f) a charge fluctuation diagram which does not contribute to spin susceptibility; (g) Landau’s interaction function.

Our many-body diagrams for the interacting susceptibility is the so-called “ladder-bubble” series as shown in Fig. 1 – this is a consistent conserving approximation for the susceptibility. Direct calculation of these diagrams turns out to be difficult for the long ranged Coulomb interaction. However, at  $T = 0$ , Landau showed that  $\chi^*$  can be equivalently expressed through the Landau’s interaction function  $f(\mathbf{k}, \mathbf{k}')$  (shown in Fig. 1(g)) as<sup>13</sup>:

$$\frac{\chi}{\chi^*} = \frac{m}{m^*} + \frac{1}{(2\pi)^2} \int f_e(\theta) d\theta, \quad (1)$$

where  $\chi$  is the Pauli spin susceptibility,  $f_e(\theta) = f_e(\mathbf{k}, \mathbf{k}')$  with  $\mathbf{k}$  and  $\mathbf{k}'$  on-shell (i.e.  $\mathbf{k}^2/2m = \mathbf{k}'^2/2m (= E_F)$ ) is the exchange part of Landau's interaction function (Fig. 1(g)(i)),  $\theta$  is the angle between  $\mathbf{k}$  and  $\mathbf{k}'$ . Similarly, the Landau theory expression for the effective mass  $m^*$  is<sup>13</sup>

$$\frac{m}{m^*} = 1 - \frac{1}{(2\pi)^2} \int f(\theta) d\theta. \quad (2)$$

Note that the spin independent exchange Landau's interaction function  $f_e(\mathbf{k}, \mathbf{k}')$  is responsible for the difference between the ratio  $\chi/\chi^*$  and  $m/m^*$ .<sup>13</sup>

An equivalent, and easier way to derive the effective mass is through calculating quasiparticle self-energy and obtaining its momentum derivative. The self-energy within RPA can be written as<sup>14</sup>

$$\Sigma(\mathbf{k}, \omega) = - \int \frac{d^2q}{(2\pi)^2} \int \frac{d\nu}{2\pi i} \frac{v_q}{\epsilon(\mathbf{q}, \nu)} G_0(\mathbf{q} + \mathbf{k}, \nu + \omega), \quad (3)$$

where  $v_q = F(q)2\pi e^2/q$  is the bare electron-electron interaction and  $F(q)$  the *quasi*-2D form factor for the electron-electron interaction<sup>2</sup> which will be described in detail later. Note that this form factor also appears in the expression of dynamical dielectric function  $\epsilon(\mathbf{q}, \nu)$  through  $v_q$ . As mentioned earlier, a significant quantitative feature of our theory is the inclusion of the realistic *quasi*-2D Coulomb interaction<sup>2</sup> in our calculation which substantially reduces (compared with the pure 2D case) the quantitative many-body renormalization effects. In Eq. (3)

$$G_0(\mathbf{k}, \omega) = \frac{1 - n_F(\xi_{\mathbf{k}})}{\omega - \xi_{\mathbf{k}} + i0^+} + \frac{n_F(\xi_{\mathbf{k}})}{\omega - \xi_{\mathbf{k}} - i0^+} \quad (4)$$

is the bare Green's function with  $n_F$  the Fermi distribution function and  $\xi_{\mathbf{k}} = k^2/(2m) - E_F$  with  $E_F$  the non-interacting Fermi energy. It is shown<sup>14</sup> that the integration along real axis in the expression of self-energy (Eq. (3)) can be deformed onto imaginary axis, which avoids the singularities along the real axis and makes the integration easier. The contour deformation also breaks the expression of self-energy into separate terms that correspond respectively to contributions from the spin-dependent and spin-independent part of the Landau's interaction function shown in Fig. 1, and is very useful for us to derive the expression for susceptibility as shown below. The expression of the real part of the self-energy can then be written as

$$\begin{aligned} \text{Re } \Sigma(\mathbf{k}, \omega) = & - \int \frac{d^2q}{(2\pi)^2} v_q \Theta(2m\omega + k_F^2 - |\mathbf{q} - \mathbf{k}|^2) \\ & + \int \frac{d^2q}{(2\pi)^2} v_q \text{Re} \frac{1}{\epsilon(\mathbf{q}, \xi_{\mathbf{q}-\mathbf{k}} - \omega)} \\ & \times \left[ \Theta(2m\omega + k_F^2 - |\mathbf{q} - \mathbf{k}|^2) - \Theta(k_F^2 - |\mathbf{q} - \mathbf{k}|^2) \right] \\ & - \int \frac{d^2q}{(2\pi)^2} \int \frac{d\nu}{2\pi} v_q \left[ \frac{1}{\epsilon(\mathbf{q}, i\nu)} - 1 \right] \frac{1}{i\nu + \omega - \xi_{\mathbf{q}+\mathbf{k}}}, \quad (5) \end{aligned}$$

where  $k_F$  is the Fermi momentum. The effective mass is derived from the expression of the real part of the quasiparticle self-energy by  $m/m^* = 1 + (m/k_F) \frac{d}{dk} \text{Re } \Sigma(\mathbf{k}, \xi_{\mathbf{k}})|_{k=k_F}$ .<sup>13</sup> Combining this with Eq. (1), we have

$$\frac{\chi}{\chi^*} = 1 + \frac{1}{(2\pi)^2} \int f_e(\theta) d\theta + \frac{m}{k_F} \frac{d}{dk} \text{Re } \Sigma(\mathbf{k}, \xi_{\mathbf{k}})|_{k=k_F}. \quad (6)$$

It is not difficult to show that the second term of Eq. (5) accounts for the contribution from the spin-independent exchange Landau's interaction function  $f_e(\mathbf{k}, \mathbf{k}')$  (Fig. 1(g)(i)), and therefore the term  $(2\pi)^{-2} \int f_e(\theta) d\theta$  in Eq. (6) exactly cancels the momentum derivative of the second term in the self-energy Eq. (5). Hence the expression of  $\chi/\chi^*$  only contains contributions from the  $k$  derivatives of the first and third term in Eq. (5). After converting all the expressions in terms of the dimensionless parameter  $r_s$ , and using  $2k_F$ ,  $4E_F$ ,  $2m$  as the momentum, energy, and mass units, the expression for  $\chi^*/\chi \equiv g^*m^*/(gm)$ , where  $\chi^*(\chi)$ ,  $g^*(g)$ ,  $m^*(m)$  are respectively the interacting (noninteracting) spin susceptibility, the Landau  $g$ -factor, and the effective mass, is given in our theory as

$$\begin{aligned} \frac{\chi}{\chi^*} = & - \frac{2\alpha r_s}{\pi} \int_0^1 dx \frac{x F(x)}{\sqrt{1-x^2}} \\ & + \frac{\sqrt{2}\alpha r_s}{\pi} \int_0^\infty x^2 F(x) dx \int_0^\infty du \left[ \frac{1}{\epsilon(x, iu)} - 1 \right] \\ & \cdot \left[ A\sqrt{1+A/R} - B\sqrt{1-A/R} \right] R^{-5/2}, \quad (7) \end{aligned}$$

where  $\alpha = \sqrt{g_v g_s/4}$  with  $g_v$  ( $g_s$ ) the valley (spin degeneracy);  $A = x^4 - x^2 - u$ ,  $B = 2xu$ ,  $R = \sqrt{A^2 + B^2}$ ;  $x = q/(2k_F)$  and  $u = \omega/(4E_F)$ ;  $\epsilon(x, iu) = 1 + \alpha r_s g_v g_s F(x) [1/(2x) - \sqrt{A+R}/(2^{3/2}x^3)]$  is the imaginary frequency dielectric function. For 2D quantum well, the form factor  $F(q)$  is given by

$$F(q) = \frac{8}{q^2 d^2 + 4\pi^2} \left[ \frac{3qd}{8} + \frac{\pi^2}{qd} - \frac{4\pi^4(1 - e^{-qd})}{q^2 d^2 (q^2 d^2 + 4\pi^2)} \right], \quad (8)$$

where  $d$  is the width of the infinite square-well potential of the quasi-2D system. For heterostructure quasi-2D systems (e.g. Si MOSFETs), the form factor is

$$F(q) = \left(1 + \frac{\kappa_{\text{ins}}}{\kappa_{\text{sc}}}\right) \frac{8 + 9qb + 3q^2 b^2}{8(1+qb)^3} + \left(1 - \frac{\kappa_{\text{ins}}}{\kappa_{\text{sc}}}\right) \frac{1}{2(1+qb)^6}, \quad (9)$$

with  $b = [\kappa_{\text{sc}} \hbar^2 / (48\pi m_z e^2 n^*)]^{1/3}$  defining the width of the quasi 2D electron gas,  $\kappa_{\text{sc}}$  and  $\kappa_{\text{ins}}$  are the dielectric constants for the space charge layer and the insulator layer,  $m_z$  is the band mass in the direction perpendicular to the quasi 2D layer, and  $n^* = n_{\text{depl}} + \frac{11}{32}n$  with  $n_{\text{depl}}$  the depletion layer charge density and  $n$  the 2D electron density. We choose  $n_{\text{depl}}$  to be zero in our calculations, since it is unknown in general (finite small value of  $n_{\text{depl}}$

do not change our results). From Eqs. (1) and (2) we have

$$\frac{m}{m^*} = \frac{\chi}{\chi^*} + \frac{\alpha r_s}{\pi} \int_0^1 dx \frac{F(x)}{x\epsilon(x,0)}. \quad (10)$$

To avoid any possible confusion, we emphasize that the definition of our spin susceptibility is the derivative of the magnetization with respect to the applied magnetic field, and therefore  $\chi^*$  is well-defined even in a non-zero parallel magnetic field  $B$ . It is important to note and easy to show that, within our approximation in which the spin-orbital effect can be neglected, the parallel field  $B$  dependence of the spin susceptibility  $\chi^*$  and the  $g$ -factor  $g^*$  manifests only through the spin-degeneracy factor  $g_s$ , which is present in the expression (7).

Motivated by recent experimental studies, we have directly evaluated the interacting susceptibility as a function of density at different spin- ( $g_s = 1, 2$ ) and valley-degeneracy ( $g_v = 1, 2$  for AlAs quantum wells) for three different 2D semiconductor systems: n-Si(100) inversion layers; n-GaAs gated undoped heterostructures; modulation-doped AlAs quantum wells. We also calculated effective mass for n-GaAs heterostructures motivated by a very recent experimental report<sup>11</sup>. In the rest of this paper, we present and discuss our calculated results for  $\chi^*/\chi$  and  $m^*/m$  in light of the recent experimental data in 2D semiconductor structures.

### III. RESULTS FOR SPIN SUSCEPTIBILITY

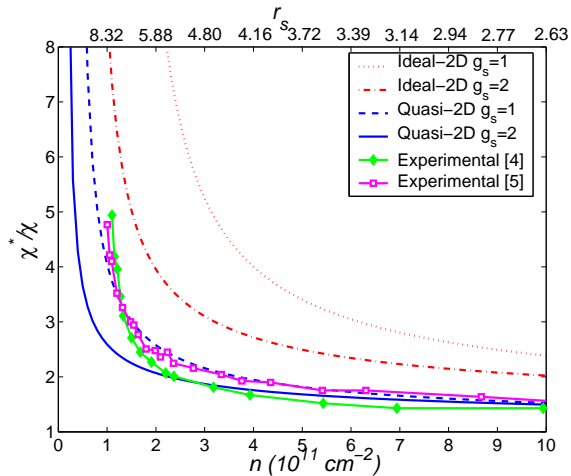


FIG. 2: (Color Online.) Calculated spin susceptibility of Si MOSFET ideal and *quasi*-2D systems with  $g_s = 1$  and 2, to be compared with experimental data from Refs. 4,5.

In Fig. 2 we show our (100) Si MOSFET results (taking a valley degeneracy  $g_v = 2$ ) for the calculated susceptibility comparing with the recent experimental results. We show two sets of results corresponding to the realistic *quasi*-2D system and the strict 2D system. In each case

we show the calculated susceptibility for both the  $g_s = 1$  (due to the presence of an external magnetic field) and the normal  $g_s = 2$  situation. Since the experiments are invariably carried out in the presence of finite external magnetic fields, the experimental results probably correspond to the region in between the  $g_s = 1$  and  $g_s = 2$  theoretical curves (for the *quasi*-2D system). A more detailed discussion is made in Sec. V on the reason why we are comparing the experimental data with our  $g_s = 1$  and  $g_s = 2$  theoretical results. There are three important points we make about Fig. 2: (1) The *quasi*-2D results are lower than the 2D results by a factor of 1.5 to 3, and the relative difference is much larger at low carrier densities since the effective *quasi*-2D layer width is larger at lower 2D densities; (2) the theory gives a reasonable description of the experimental data, – in particular, the experimental data points lie very close to the region between the theoretical  $g_s = 1$  and  $g_s = 2$  *quasi*-2D susceptibility results; (3) the pure-2D results disagree with experiments.

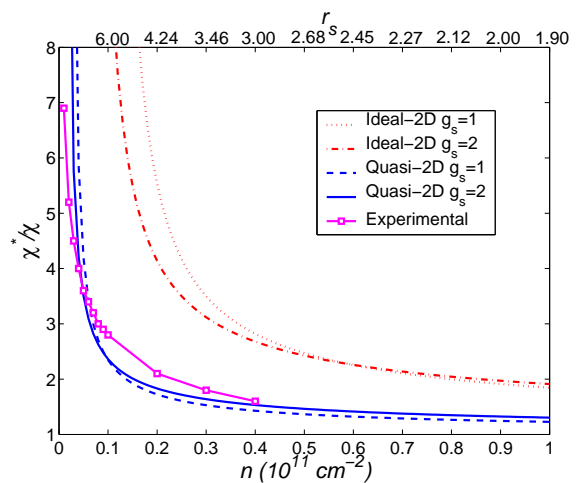


FIG. 3: (Color online.) Calculated spin susceptibility of GaAs heterostructure ideal and *quasi*-2D systems with  $g_s = 1$  and 2, to be compared with experimental data from Refs. 7.

In Fig. 3 we show our theoretical susceptibility results for electrons confined in *quasi*-2D GaAs heterostructure (valley degeneracy  $g_v = 1$ ) comparing with the recent measurements of Zhu *et. al.*<sup>7</sup>. Again, the agreement between our results and the experimental measurements is very good for the realistic *quasi*-2D calculations. Note that at the low carrier densities of interest in the GaAs 2D system, the *quasi*-2D effects are extremely strong (almost a factor of 5!), and the quantum Monte Carlo (QMC) calculation<sup>15</sup> with which the experimental results were compared in Ref. 7 are completely inapplicable since they are for a strict 2D system rather than a *quasi*-2D system. In fact, any agreement between the measured susceptibility and the QMC results for the ideal zero-width 2D system should be taken as a spectacular quantitative failure for the QMC theory in the low-density regime. The reason for such a strong *quasi*-2D effect in GaAs is that at

very low densities ( $n \sim 10^9 \text{cm}^{-2}$ ), the transverse *quasi*-2D width of the electron wavefunction is extremely large ( $> 500 \text{\AA}$ ) so that the Coulomb interaction is substantially suppressed compared with the strict 2D limit result. (This demonstrates that it is misleading to compare *quasi*-2D experimental results with the strict 2D theory as is often done in the literature!).

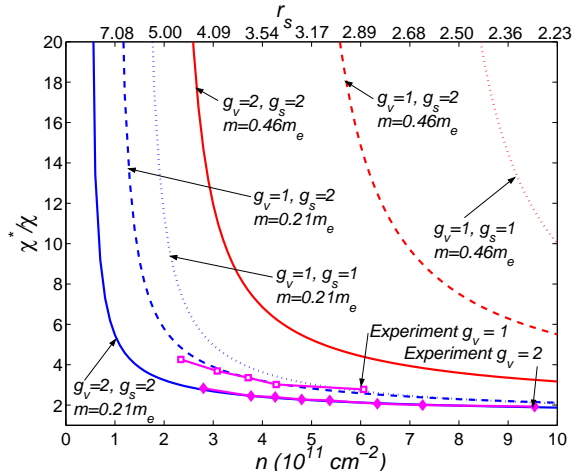


FIG. 4: (Color online.) Calculated spin susceptibility of AlAs quantum well ideal and *quasi*-2D systems with  $g_s = 1$  and  $2$  and  $g_v = 1$  and  $2$ , to be compared with experimental data from Refs. 9. Effective  $\kappa = 10$ . We use two different values of band mass:  $m = 0.21m_e$  and  $m = 0.46m_e$ .

In Fig. 4 we show our theoretical results for AlAs quantum wells. The AlAs quantum wells used in Ref. 8,9 are rather narrow (width  $\sim 50 \text{\AA}$ ), and the additional self-consistent confining potential arising from the 2D electrons themselves produces even stronger confinement of the carriers thus further narrowing the effective *quasi*-2D width. Therefore, we show only the strict-2D results for the 2D AlAs system in Fig. 4 for the sake of clarity. Our corresponding *quasi*-2D results are somewhat below the theoretical curves for the strict-2D case. In Fig. 4 we show our theoretical results for two different valley degeneracy ( $g_v = 1$  and  $2$ ) situations. Our theoretical investigation of the valley degeneracy dependence of the 2D spin susceptibility behavior is necessitated by the puzzling recent experimental findings<sup>8,9</sup> of an interesting valley degeneracy dependence in AlAs systems, namely, the many-body enhancement for  $\chi^*/\chi$  is larger for the valley occupancy of 1 than the valley occupancy of 2. (Our results for Si MOSFETs and GaAs heterostructures in Figs. 1 and 2 are for valley degeneracy values  $g_v = 2$  and  $1$  respectively, consistent with the known band structure for Si and GaAs.)

In Fig. 4, the results for  $m = 0.21m_e$ , which corresponds to the transverse AlAs band mass  $m_t$ , are in reasonable quantitative agreement with the experimental AlAs quantum well results, including the anomalous finding of  $\chi^*/\chi$  having a stronger many-body Fermi liquid enhancement for the lower valley occupancy of 1 than

for the higher occupancy of 2. We note that at high enough electron densities ( $\gtrsim 10^{12} \text{cm}^{-2}$ ), this anomalous valley dependence of the spin susceptibility would disappear according to our theoretical calculations with  $\chi^*/\chi$  for  $g_v = 2$  being larger than that for  $g_v = 1$ , consistent with one's naive expectations. It may be more appropriate to use<sup>16</sup> a larger 2D band mass in our calculation given by  $m = 0.46m_e = \sqrt{m_t m_l}$  with  $m_l = m_e$  the longitudinal band mass. Use of this band mass results in larger theoretical values for spin susceptibility than that was measured in experiment, but the trend and the characteristic of valley-degeneracy dependence remains the same. The exact cause of the quantitative difference between our  $m = 0.46m_e$  results and the experiments probably lies in the yet unknown details of the samples and experimental procedures, and are therefore not clear to us right now.

Why does the valley occupancy dependence of the many-body susceptibility enhancement act in such a way? The reason lies in many-body correlation effects beyond the naive exchange energy considerations. Within an exchange-only Hartree-Fock theory, in fact, the 2-valley occupancy state would have a higher susceptibility enhancement than the 1-valley state. But correlation effects are important in the system, and at low enough carrier densities the 1-valley state turns out to have stronger many-body effects than the 2-valley state. Our theory, which is essentially a self-consistent dynamically screened Hartree-Fock theory, includes correlation effects demonstrating that at low enough carrier densities,  $\chi^*/\chi$  could be enhanced in the 1-valley state over the 2-valley state as has been experimentally observed. Another way to understand this is through the screening effect. As  $g_v$  increases, Fermi momentum decreases as  $k_F \propto 1/\sqrt{g_v}$ , which favors many-body renormalization. However, the screening effect increases with increasing  $g_v$  since  $q_{TF} \propto g_v$ , which tends to decrease the renormalization effect. These two effects are competing with each other. At low densities, the screening effect is predominant, and therefore a smaller  $g_v$  results in much less screening than a bigger  $g_v$  and hence produces larger susceptibility renormalization. On the other hand, at high densities the screening effect is less important, and a smaller  $g_v$  results in a larger Fermi energy and a smaller renormalization effect. In particular, the valley degeneracy dependence of many-body effects should qualitatively correlate with the dimensionless parameter  $q_{TF}/(2k_F) \propto g_v^{3/2}$ : for large (small)  $q_{TF}/(2k_F)$ , low (high) density, smaller (larger) values of  $g_v$  produce larger renormalization. Note that the experimental results in Ref. 9 do not show any strong  $g_s$  dependence in contrast to our theoretical results in Fig. 4. We discuss this puzzle in Sec. V below of our paper.

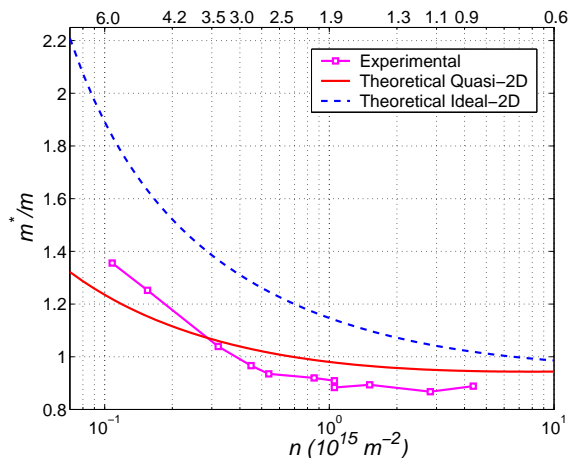


FIG. 5: (Color online.) Calculated effective mass of GaAs heterostructure ideal and *quasi*-2D systems with  $g_s = 2$  and  $g_v = 1$ , to be compared with experimental data from Refs. 11.

#### IV. RESULTS FOR EFFECTIVE MASS

Although the main task of our current work is the calculation of interacting 2D susceptibility to compare with the recent experimental results<sup>3,4,5,6,7,8,9,10</sup>, a very recent experimental report<sup>11</sup> of 2D n-GaAs effective mass measurement allows us to apply our recently developed theory<sup>14</sup> for the quasiparticle effective mass enhancement to 2D GaAs in order to compare with these experimental results. For details on the quasiparticle effective mass theory we refer to our recent publication<sup>14</sup>.

In Fig. 5 we show our theoretical effective mass results for electrons confined in *quasi*-2D GaAs heterostructure (valley degeneracy  $g_v = 1$ ) comparing with the recent measurements of Tan *et al.*<sup>11</sup>. The agreement between our results and the experimental measurements is very good for the realistic *quasi*-2D calculation. Again the ideal-2D effective mass results turn out to be much larger than the experimental data, emphasizing once more the importance of the *quasi*-2D effect on the many-body renormalization of physical quantities in such systems. We emphasize that, while at high densities the quasi-2D results are rather close (with a 10 – 20% difference) to the pure 2D results, at low densities this difference could be as large as a factor 2.

#### V. DISCUSSION

Before concluding we make some critical observations and comments on our theory and its implications and, more particularly, on the comparison with the recent experimental results. One of our important conclusions is that the inclusion of *quasi*-2D form factor effects is essential in understanding the 2D susceptibility results. As such, an important issue is the realistic nature of our model where we have included the *quasi*-2D form-factor

effects through the standard variational approximation<sup>2</sup> for heterostructures. We believe that our *quasi*-2D electronic structure model is extremely reasonable, but some uncertainty and error probably arise (particularly at low carrier densities) from our lack of knowledge about the depletion charge density in these systems.

A rather important factor in the comparison with the experimental data that is left out of our consideration is the effect of orbital coupling<sup>17</sup> of the in-plane component of the external magnetic field invariably present in the experimental measurement of the spin susceptibility. At low carrier densities, when the *quasi*-2D width of the 2D layer is large, such a magneto-orbital coupling could have substantial effects on the 2D effective mass<sup>17</sup>. This effect is, however, entirely of one-electron origin, and we assume, somewhat uncritically at this stage, that the magneto-orbital effect drops out of the susceptibility enhancement factor  $\chi^*/\chi$  since the enhancement involves a ratio of the interacting and the non-interacting effective mass both of which will be affected in a similar manner by the magneto-orbital effect. In any case, the magneto-orbital effect is negligibly small for Si MOSFETs and AlAs quantum wells because of their tight *quasi*-2D confinement, and in the n-GaAs structure the *ratio*  $\chi^*/\chi$  should not be much affected by the magneto-orbital coupling. Only at rather low densities in GaAs heterostructures the magneto-orbital effect may play a role.

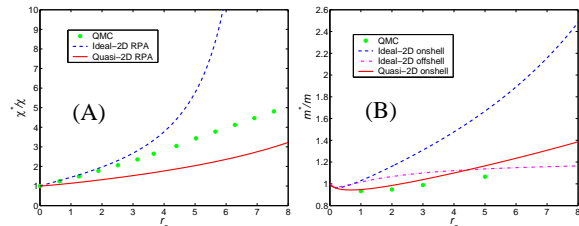


FIG. 6: (Color online.) (A) Comparison between the results of spin susceptibility calculated using QMC method<sup>15</sup> and our results calculated within RPA for a 2D electron system with  $g_s = 2, g_v = 1$ . Our results are for both ideal and quasi-2D systems as shown; the QMC results are for ideal 2D systems. (B). Comparison between our RPA many-body theory and the QMC results<sup>18</sup> for quasiparticle effective mass. Results are shown for strict 2D (both on-shell and off-shell RPA self-energy approximations as well as QMC) and quasi-2D (on-shell RPA self-energy approximation) cases. Our effective mass results shown in Fig. 5 correspond to the on-shell approximation which is the consistent approximation for the Fermi liquid effective mass within the RPA self-energy approximation.

Although our *quasi*-2D model is reasonably realistic and accurate, our many-body spin susceptibility calculation is necessarily based on approximations since the problem of an interacting quantum Coulomb system cannot be solved exactly. We emphasize in this respect that QMC calculations, while being accurate as a matter of principle, turn out as a matter of practice to be often unreliable due to various approximations (e.g. node fix-

ing, back-flow correlations, etc.) and inaccuracies (e.g. finite size effects, numerical errors) inherent in the QMC technique. Also the QMC calculations leave out *quasi*-2D effects, and are therefore quantitatively incorrect. In Fig. 6 we make a comparison between our result and the QMC result<sup>15</sup> for susceptibility in an ideal-2D electron system with  $g_s = 2$  and  $g_v = 1$ . In the intermediate and large  $r_s$  region, the difference between the results of RPA and QMC methods turn to be very large. But we note that our *quasi*-2D results are quantitatively quite close to the QMC pure-2D results. (A similar situation seems to hold for the effective mass calculations also.) This demonstrates the care that is needed in comparing theory with experiments in this problem.

In comparing theory and experiment for the susceptibility and the effective mass in 2D electron systems it is important to emphasize the fact that the experimental measurements for  $\chi^*$  and  $m^*$  in 2D systems are typically *not* thermodynamic measurements, but are essentially transport measurements of thermodynamic quantities in an applied magnetic field which spin-polarizes the system through the Zeeman splitting. For example, the 2D susceptibility is measured<sup>3,4,5,6,7,8,9,10</sup> by either monitoring<sup>3</sup> the full spin polarization of a 2D system in an applied parallel field or through the clever coincidence technique<sup>12</sup> in a tilted magnetic field. We want to raise three important issues related to these experimental techniques and their relevance to our theory. First, strictly speaking these techniques does not provide a true measurements of the spin susceptibility  $\chi^*$  that is defined through  $\chi^*(B) = \partial M / \partial B$  with  $M$  the magnetization and  $B$  the applied magnetic field. In all these techniques, the experimentally measured quantity is actually  $M/B$ , which we now call  $\tilde{\chi}^*(B)$ . As has been explained in the experimental literature<sup>3,4,5,6,7,8,9</sup>, these studies measure indirectly the occupancies of spin up and down levels through transport or Landau level coincidence measurements. The spin susceptibility is then inferred from these indirect spin polarization studies by using the simple non-interacting spin-dependent density formula: In the transport measurement technique,  $g^* \mu_B B_p = E_F$  where  $B_p$  is the so-called saturation (parallel) field for ‘complete spin polarization’. In the Landau level coincidence technique,  $g^* \mu_B B = i \omega_c = i e \hbar B_{\perp} / m^*$  with  $i$  half integer or integer. In either case, the derived spin susceptibility is exactly  $\tilde{\chi}^*(B) = M/B$  that we have just discussed. ( $B = B_p$  in the transport measurement technique, and  $B$  corresponds to the Landau level coincidence magnetic field in the Landau level coincidence technique.) It is important to note that  $\tilde{\chi}^*(B) \neq \chi^*(B) \neq \chi^*(B = 0)$  for  $B \gg 0$ , and these three quantities coincide in the  $B \rightarrow 0$  limit. The precise definition of spin susceptibility was never explicitly made clear in the previous experimental literature. Second, even though the experimentally observed  $\tilde{\chi}^*(B)$  is not exactly the thermodynamic quantity  $\chi^* = \chi^*(B = 0)$ , in normal circumstances they are close to each other. Especially, if the magnetization curve of the system is smooth (which normally it will

be),  $\tilde{\chi}^*(B)$  is in between  $\chi^*(B = 0)$  and  $\chi^*(B = B_p)$  which are the two extreme case we are considering in this work. As we mentioned before, since the magnetic field dependence of  $\chi^*$  only manifests itself through the spin degeneracy factor, we can say that the experimentally measured  $\tilde{\chi}^*(B)$  should be in between  $\chi^*(g_s = 2)$  and  $\chi^*(g_s = 1)$ , which is the justification for our comparison of the experimental data with our  $g_s = 1, 2$  theoretical results. In Ref. 7, the issue of finite field and hence the spin degeneracy factor dependence of the susceptibility is made more clear. However, in this case not only the partial spin polarization need to be considered, the effect of the finite perpendicular magnetic field and Landau levels on the susceptibility need to be further investigated, which is beyond the scope of this work. Third, the difference between  $\tilde{\chi}^*(B)$  and  $\chi^*$  may be helpful in understanding some of the discrepancies between the experimental data and our theoretical findings. For example the recent measurements<sup>8,9</sup> in 2D AlAs quantum well systems find a strongly valley-degeneracy-dependent spin susceptibility which, however, demonstrates essentially *no* spin degeneracy dependence. Since the valley index is essentially a pseudo-spin index, theory would predict the *same* valley and spin degeneracy dependence of susceptibility unless there is strong spin-orbit or valley-orbit band structure effects in the system. Therefore, in the  $r_s$  region where the spin susceptibility has a large dependence on the valley degeneracy, the spin degeneracy should play an equally big role, as shown in Fig. 4. This theory-experimental discrepancy may very well be a result of the difference between  $\tilde{\chi}^*(B)$  and  $\chi^*$ . This factor might have also caused the quantitative discrepancy between our RPA results (using  $m = 0.46m_e$ ) and the experimental results shown in Fig. 4. Other possible explanation could also lie in one-electron band structure physics, not in many-body theory. There have been no QMC calculations revealing the spin and valley degeneracy dependency of the spin susceptibility.

The many-body approximation we use in our work, namely the renormalized interaction calculated within the infinite series of bubble diagrams and the susceptibility calculated in the infinite series of ladder diagrams using the appropriate dynamically screened interaction (i.e. the ladder-bubble approximation for  $\chi^*$ ), corresponds to the leading-order expansion in the dynamically screened interaction. Such an expansion is asymptotically exact in the high-density limit, and is known to work well in the low-density limit as well. Unfortunately, its regime of quantitative validity is unknown, and it is likely to become progressively quantitatively inaccurate as  $r_s$  increases. It should, however, be qualitatively valid for larger  $r_s$  values as long as the interacting electron system remains a Fermi liquid. Our reasonable agreement (without adjusting any parameters) with existing experiments shows that the theory remains well-valid in 2D-systems at least up-to  $r_s \sim 7$ , which is consistent with the success of the corresponding 3D theory in the metallic densities ( $r_s \sim 3-6$ ). Since no systematic and uncontrolled many-

body theory approximation is available for susceptibility beyond the ladder-bubble series approximation carried out in this paper, we can only test the validity of our theory through the direct comparison with experiments, and on this ground the theory seems to be well-justified.

Our quasiparticle effective mass results (Fig. 5) are based on the theory developed by us in Ref. 14 recently. This theory is the RPA theory, based on the leading-order self-energy calculation in the dynamically screened Coulomb interaction. While the theory is asymptotically exact in the high density  $r_s \rightarrow 0$  limit, it is not based on an  $r_s$  expansion and is essentially a self-consistent field theory. Unfortunately, however, like many other self-consistent field theories, the level of validity of this theory for large  $r_s$  (i.e. the strongly interacting regime) is unknown except that it is expected to remain qualitatively valid<sup>1,13,14</sup> for  $r_s > 1$  unless there is a quantum phase transition. Since we have discussed the approximation scheme and the validity of our RPA effective mass theory in some details in Ref. 14, we do not repeat those arguments here. We point out that the effective mass results given in Fig. 5 use the “on-shell” self-energy approximation<sup>13,14</sup>, which has been argued<sup>13,14</sup> to be the correct dynamical approximation consistent with the Landau Fermi liquid theory as long as the self-energy is obtained in the leading-order dynamically screened interaction (i.e. RPA). Our “off-shell” approximation for the 2D effective mass (shown in Fig. 6(B)) differs from the corresponding “on-shell” results by a factor of 2 or more at low densities, and show different trends as well. The fact that the “on-shell” effective mass results agree much better with experiment than the “off-shell” results is additional evidence in support of the “on-shell” approximation being the correct one within RPA self-energy scheme. One can try to “improve” upon RPA by including local field corrections<sup>19</sup> to the dynamical electron polarizability (i.e. bare bubble of RPA) which, in some crude manner, simulates the incorporation of higher-order vertex corrections in the theory. But such local field corrections are uncontrolled, and probably inconsistent, since many diagrams in the same order are typically left out. We are therefore unconvinced that the inclusion of local field corrections in the theory is necessarily an improvement on RPA. The great conceptual advantage of RPA is that it is a well-defined approximation that is both highly physically motivated (i.e. dynamical screening) and theoretically exact in the high-density ( $r_s \rightarrow 0$ ) limit. Attempted improvement upon RPA through the arbitrary inclusion of local field correction may neither be theoretically justifiable nor more reliable. Keeping these caveats in mind, we mention that several previous works<sup>14,19</sup> have shown that local field corrections to the many-body properties of two dimensional electron gas turn to be very small in the density range of our current interest.

It has recently been discussed in detail by us<sup>14</sup> that RPA is not necessarily a high-density theory although it is exact in the high density limit. The ring diagram

approximation, which is at the heart of RPA, is an expansion in the dynamically screened interaction. Under some circumstance RPA can be very loosely thought of<sup>1,14</sup> as an expansion in an effective parameter  $r_s/(r_s + C)$  where  $C > 1$  is a constant. This implies that RPA could in some situation turn out to be decent approximation in the  $r_s > 1$  case. Indeed 3D metals, with  $3 < r_s < 6$ , seem to be reasonably well-described<sup>1</sup> by RPA. Leading-order vertex corrections to RPA<sup>13,14,19</sup> typically produce only small quantitative corrections in the  $r_s > 1$  regime, again empirically justifying the validity of RPA. There is obviously a lot of cancellation among the higher-order diagrams (in particular, between the self-energy and the vertex diagrams) leading to the good empirical success of RPA consisting only of the bare bubble diagrams. But this empirical success is physically well-motivated, arising from the long-range nature of the inter-electron Coulomb interaction with the decisive point of physics being the dynamical screening properties of a Coulomb liquid. In an interacting system with short-range bare interactions, e.g. neutral He-3, the ring-diagrams play no special role, and RPA is not a meaningful approximation. In a strongly interacting system, such as a 2D electron system with  $r_s > 1$ , one must use a careful and critical comparison between theory and experiment as the principal guide in deciding the validity of any theory. By this standard RPA appears to be a reasonable approximation even for  $r_s > 1$ . There are many other theoretical techniques in condensed matter physics which work well beyond their putative regime of validity – for example, the dynamical mean field theory (DMFT), which is exact in infinite dimensions, seems to provide good results in 2 and 3 dimensional strongly correlated systems, and the local density approximation (LDA), which is exact for very slowly varying density inhomogeneity, works well for the band structure of real solids with their rapidly varying densities. Similar to DMFT and LDA, RPA works well because it is fundamentally a non-perturbative theory which accounts for some key ingredient of the interaction physics, namely, screening in the situation under consideration in this paper.

We conclude by emphasizing that the most significant implication of the excellent qualitative and quantitative agreement between our theory and 2D spin susceptibility and effective mass measurements is that interacting 2D electron systems, which have been of much interest recently, remain Fermi liquids down to reasonably low carrier densities ( $r_s \sim 7$  or so at least), and many-body perturbative techniques, coupled with a realistic *quasi*-2D description for the electronic structure, provide a very good qualitative and quantitative model for these systems. There is no need to invoke any non-Fermi liquid concepts to explain the recent experimental results on quasiparticle renormalization effects<sup>3,4,5,6,7,8,9,10,11</sup>.

This work is supported by the NSF, the DARPA, the US-ONR, and the LPS.

- 
- <sup>1</sup> L. Hedin and S. Lundqvist, *Solid State Physics* (Academic Press, New York and London), **23**, 2 (1969), and references therein.
- <sup>2</sup> T. Ando, A. B. Fowler, and F. Stern, *Rev. Mod. Phys.* **54**, 437 (1982), and references therein.
- <sup>3</sup> T. Okamoto, K. Hosoya, S. Kawaji, and A. Yagi, *Phys. Rev. Lett.* **82**, 3875 (1998).
- <sup>4</sup> A. Shashkin, S. V. Kravchenko, V. T. Dolgoplov, and T. M. Klapwijk, *Phys. Rev. Lett.* **87**, 086801 (2001).
- <sup>5</sup> V. M. Pudalov, M. E. Gershenson, H. Kojima, N. Butch, E. M. Dizhur, G. Brunthaler, A. Prinz, and G. Bauer, *Phys. Rev. Lett.* **88**, 196404 (2002).
- <sup>6</sup> E. Tutuc, S. Melinte, and M. Shayegan, *Phys. Rev. Lett.* **88**, 036805 (2002).
- <sup>7</sup> J. Zhu, H. L. Stormer, L. N. Pfeiffer, K. W. Baldwin, and K. W. West, *Phys. Rev. Lett.* **90**, 056805 (2003).
- <sup>8</sup> K. Vakili, Y. P. Shkolnikov, E. Tutuc, E. P. D. Poortere, and M. Shayegan, *Phys. Rev. Lett.* **92**, 226401 (2004).
- <sup>9</sup> Y. P. Shkolnikov, K. Vakili, E. P. D. Poortere, and M. Shayegan, *Phys. Rev. Lett.* **92**, 246804 (2004).
- <sup>10</sup> A. A. Shashkin, M. Rahimi, S. Anissimova, S. V. Kravchenko, V. T. Dolgoplov, and T. M. Klapwijk, *Phys. Rev. Lett.* **91**, 046403 (2003).
- <sup>11</sup> Y.-W. Tan, J. Zhu, H. L. Stormer, L. N. Pfeiffer, K. W. Baldwin, and K. W. West, cond-mat/0412260.
- <sup>12</sup> F. Fang and P. J. Stiles, *Phys. Rev.* **174**, 823 (1968).
- <sup>13</sup> T. M. Rice, *Ann. Phys. (N. Y.)* **31**, 100 (1965).
- <sup>14</sup> Y. Zhang and S. Das Sarma, *Phys. Rev. B* **70**, 035104 (2004); Y. Zhang and S. Das Sarma, *Phys. Rev. B* **71**, 045322 (2005); Y. Zhang, V. M. Yakovenko and S. Das Darma, *Phys. Rev. B* **71**, 115105 (2005).
- <sup>15</sup> C. Attacalite, S. Moroni, P. Gori-Giorgi, and G. B. Bachelet, *Phys. Rev. Lett.* **88**, 256601 (2002), and references therein.
- <sup>16</sup> M. Shayegan, private communications.
- <sup>17</sup> S. Das Sarma and E. H. Hwang, *Phys. Rev. Lett.* **84**, 5596 (2000); see also E. Tutuc, S. Melinte, E. P. De Poortere, M. Shayegan and R. Winkler, *Phys. Rev. B* **67**, 241309 (2003).
- <sup>18</sup> Y. Kwon, D. M. Ceperley, and R. M. Martin, *Phys. Rev. B* **50**, 1684 (1994).
- <sup>19</sup> I. K. Marmorosk and S. Das Sarma, *Phys. Rev. B* **44**, R3451 (1991).